

Synthesis, Structure and Fluorescence Property of New Cd-MOFs Based on a Tetraphenylethylene (TPE) Ligand^①

LIANG Yu XU Xiu-Dian NI Jian-Ling

LI Jun-Feng WANG Fang-Ming^②

(School of Environmental and Chemical Engineering,

Jiangsu University of Science and Technology, Zhenjiang 212003, China)

ABSTRACT A very stable Cd^{II}-organic framework, $\{[\text{Cd}_3(\text{Tipe})_{1.5}(\text{bpodc})_2\text{Cl}_2](\text{H}_2\text{O})_2\}_n$ (compound **1**, Tipe = 1,1,2,2-tetrakis(4-(imidazol-1-yl)phenyl)ethene, bpodc = benzophenone-4,4-dicarboxylic acid), has been successfully synthesized under hydrothermal conditions. Compound **1** crystallizes in the triclinic system, space group $P\bar{1}$, with $a = 12.289(3)$, $b = 15.951(4)$, $c = 20.755(5)$ Å, $\alpha = 81.248(2)^\circ$, $\beta = 83.905(2)^\circ$, $\gamma = 89.452(2)^\circ$; $V = 3998.2(17)$ Å³, $Z = 2$, $M_r = 1839.59$, $D_c = 1.528$ g/cm³, $\mu = 0.925$ mm⁻¹, $F(000) = 1844$, $R = 0.0508$ and $wR = 0.1571$ for 13998 observed reflections ($I > 2\sigma(I)$). Its overall structure is a three-dimensional stacking with a porosity of 10.1% based on a calculation by PLATON. Compound **1** shows a blue fluorescence emission with the peak maximum of 501 nm ($\lambda_{\text{ex}} = 397$ nm) by ligand-to-ligand charge transfer of TPE chromophore. And it exhibits excellent performance in detecting Fe³⁺ and Cr₂O₇²⁻ ions in aqueous solutions as a multi-response sensor.

Keywords: tetraphenylethane, sensor, luminescent, metal-organic framework;

DOI: 10.14102/j.cnki.0254-5861.2011-2794

1 INTRODUCTION

In recent years, metal-organic frameworks (MOFs), a fascinating class of hybrid porous materials, have attracted great attention thanks to their unique structural features and potential applications in various fields^[1-3]. Among them, luminescent MOFs (LMOFs) have drawn extensive attention because of their easily introducing light-emitting building blocks and potential applications in light-emitting devices^[4-7], chemical sensing^[8-11], and photocatalysis^[12, 13].

Tetraphenylethylene (TPE) and its derivatives are prominent luminescent material with aggregation-induced emission (AIE) characteristics^[14, 15]. TPE can fluoresce intensely and make main contributions to the emissions of LMOFs^[16, 17]. The strong emissions enable TPE-based MOFs to serve as promising luminescent sensors by a signal-off mode^[18, 19].

Based on our former researches on LMOFs with AIE effect^[20, 21], herein, we successfully constructed a new 3D metal-organic framework $\{[\text{Cd}_3(\text{Tipe})_{1.5}(\text{bpodc})_2\text{Cl}_2](\text{H}_2\text{O})_2\}_n$ from

a TPE-core ligand. It also shows good AIE luminescence property. And its structure, X-ray powder diffraction (XRPD), and thermogravimetric analyses (TGA) were also investigated.

2 EXPERIMENTAL

2.1 Materials and instruments

All chemical reagents and materials of AR grade were obtained from commercial companies and used without further purification. The ligand Tipe was synthesized as the route of reference^[22, 23]. Single-crystal X-ray diffraction (SXRD) data were collected by a Bruker SMART APEX II CCD-based diffractometer with graphite-monochromatic MoK α radiation ($\lambda = 0.71073$ Å). Infrared spectra were recorded on a Nicolet FT-1703X spectrometer in the range of 4000~500 cm⁻¹ (Fig. S1). The luminescence spectra were recorded with a spectra fluorometer FS5 at room temperature. An Ultima IV was utilized for the collection of powder X-ray

Received 2 March 2020; accepted 15 May 2020 (CCDC 1972701)

① Supported by the National Natural Science Foundation of China (No. 21671084), and a Start-up grant and pre-research foundation from Jiangsu University of Science and Technology of China

② Corresponding author. E-mail: wangfmzj@just.edu.cn

diffraction (PXRD) patterns with Cu- $K\alpha$ ($\lambda = 1.5406 \text{ \AA}$) radiation field-emission at 40 kV and 40 mA. Infrared spectra were recorded on a SHIMADZU IR prestige-21 FTIR-8400S spectrometer in the range of $4000\sim 500 \text{ cm}^{-1}$ with samples in the form of KBr pellets (Fig. S1). Thermogravimetric analyses (TGA) were conducted on a NETZSCH TG 209 F3 thermogravimeter at a heating rate of 10 K/min in a N_2 atmosphere.

2.2 Synthesis of Cd-MOF (1)

$\text{Cd}(\text{ClO}_4)_2 \cdot 6\text{H}_2\text{O}$ (0.04 mmol, 16.8 mg), Tipe (0.01 mmol, 5.96 mg), bpdc (0.02 mmol, 5.4 mg), methanol (2 mL), and H_2O (1 mL) were sealed in a glass tube and kept at 160°C for two days. Colorless crystals of the compound were obtained at a yield of 51% based on Tipe.

2.3 Single-crystal X-ray structure determination

Single-crystal reflection data for compound **1** were collec-

ted at room temperature on a Bruker SMART APEX CCD area-detector diffractometer equipped with a graphite-monochromated $\text{MoK}\alpha$ radiation ($\lambda = 0.71073 \text{ \AA}$). Empirical absorption correction was applied by using SADABS. The structure was solved by direct methods and refined by full-matrix least-squares on F^2 using the SHELXL and Olex2 programs. All non-hydrogen atoms were refined anisotropically. Hydrogen atoms were placed in calculated positions with isotropic displacement parameters set to $1.2U_{eq}$ of the attached atom.

3 RESULTS AND DISCUSSION

3.1 Crystal structure description

The cell parameters of compound **1** have been described in the abstract. And the selected bond lengths are listed in Table 1.

Table 1. Selected Bond Lengths (\AA) of Compound **1**

Bond	Dist.	Bond	Dist.	Bond	Dist.
Cd(1)–O(1)	2.216(46)	Cd(2)–N(9)	2.215(43)	Cd(3)–O(9)	2.386(61)
Cd(1)–N(1)	2.281(51)	Cd(2)–O(2)	2.246(39)	Cd(3)–O(10)	2.351(6)
Cd(1)–N(3)	2.296(47)	Cd(2)–O(3)	2.233(43)	Cd(3)–Cl(2)	2.423(22)
Cd(1)–N(5)	2.345(47)	Cd(2)–O(4)	2.564(50)	Cd(3)–Cl(3)	2.430(29)
Cd(1)–N(7)	2.240(58)	Cd(2)–O(6)	2.215(39)	Cd(3)–N(12)	2.273(49)

As shown in Fig. 1a, there are three different coordination environments for cadmium atoms. This means that cadmium atom has two coordination modes, named primary building units (PBUs) and secondary building units (SBUs). The PBU is CdO_2NCl_2 and SBU is $\text{Cd}_2\text{O}_5\text{N}_5$. In PBUs, each cadmium atom (Cd(3)) is connected with two O atoms from one bpdc linker, two Cl atoms from metal salt and one N atom from one Tipe linker to form a five-coordinated environment. Different from the coordination environment of cadmium atoms in PBUs, there exist binuclear cadmium atoms in SBUs. One cadmium atom (Cd(1)) is in a five-coordinated environment composed by four N and one O atoms. And the

other cadmium atom (Cd(2)) is also in a five-coordinate environment built by four O and one N atoms. These binuclear cadmium atoms are bound by double carboxylate bridges from different bpdc linkers. PBUs and SBUs are connected by bpdc to form a single 3D network. The bond lengths of Cd–N, Cd–Cl and Cd–O ranged from 2.281 to 2.345 \AA , 2.423 to 2.430 \AA and 2.214 to 2.564 \AA , respectively (Table 1). Cd atoms are linked with bpdc ligands to form a 1D zigzag chain along the *b*-axis. Then these 1D zigzag chains are connected into a 2D layer linked by Tipe ligands, and further stacked to a 3D supramolecular network (Fig. 1b).

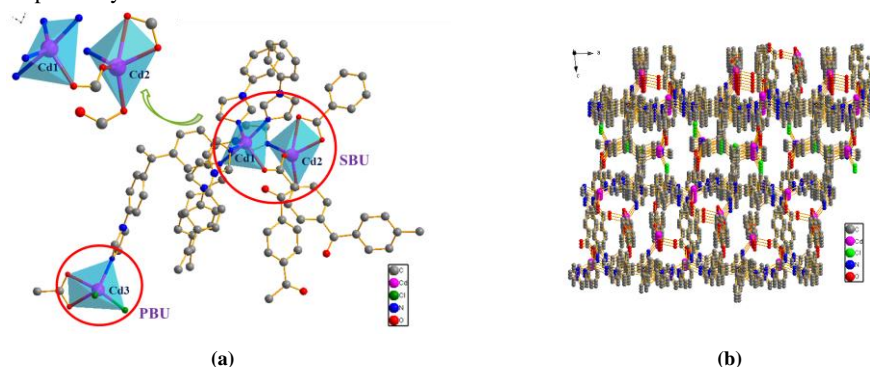


Fig. 1. (a) Coordination environment of the Cd(II) in compound **1**. (b) 3D network of **1** along the *b* axis

3.2 XRPD and TG analyses

The powder XRD patterns were performed using an Ultima IV with Cu-K α ($\lambda = 1.5406 \text{ \AA}$) radiation. The experimental

results show that the peak positions of the crystalline samples of **1** closely match those in the simulation from single-crystal data, showing the phase purity of the as-made samples (Fig. 2).

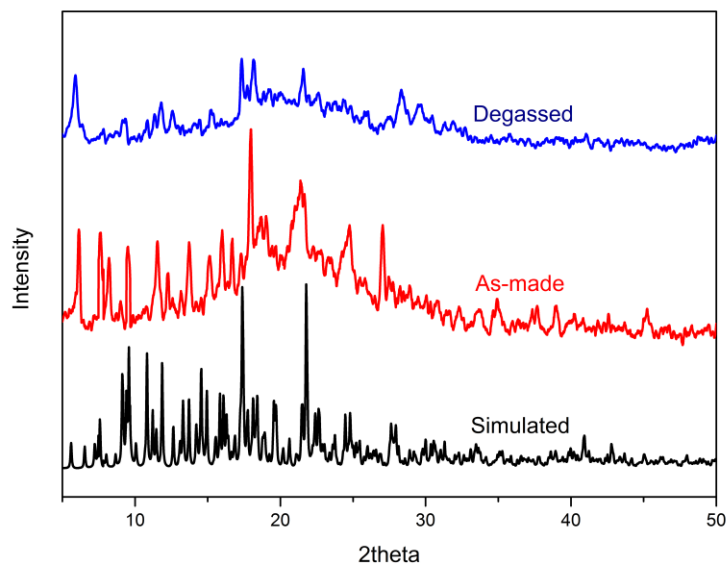


Fig. 2. Powder X-ray diffraction patterns of compound **1**

Thermogravimetric analysis (TGA) was recorded on compound **1** to test their thermal stability from 15 to 800 °C under nitrogen atmosphere (Fig. 3). The result of TGA curve indicates that the solvent molecules in the holes were removed from room temperature to 100 °C. It is known that

1 $\{[\text{Cd}_3(\text{Tipe})_{1.5}(\text{bpdc})_2\text{Cl}_2] (\text{H}_2\text{O})_2\}$ loses 2% of 2 free water molecules. And the mass loss from 100 to 250 °C is 9.47% owing to the escape of Cl^- . When the temperature increases to 350 °C, a quick mass loss is observed, which may correspond to the decomposition of the framework.

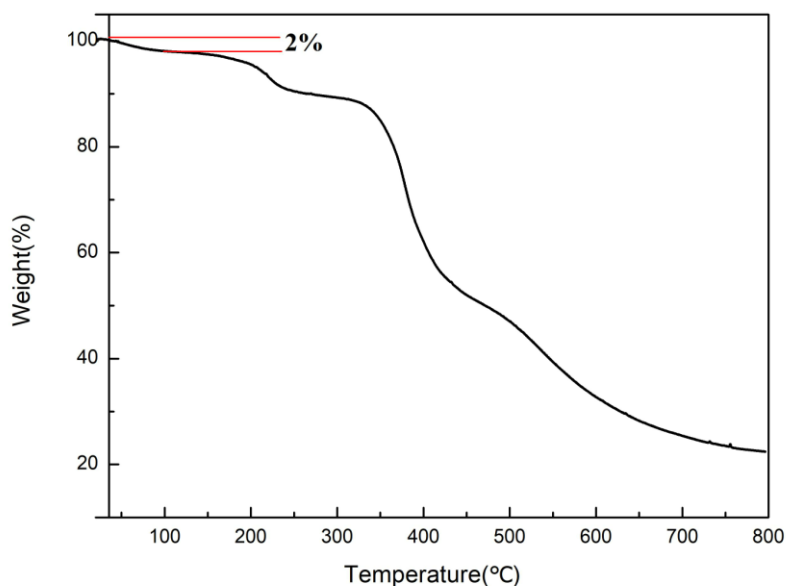
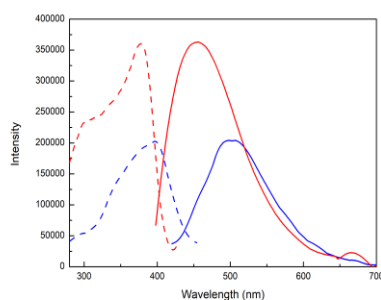


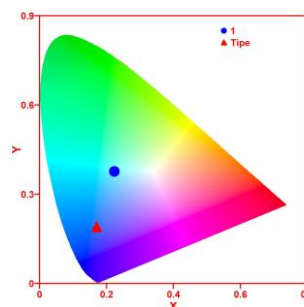
Fig. 3. TG curve of compound **1** and tipe

3.3 Fluorescence properties

The luminescent properties of compound **1** were studied at room temperature in solid state (Fig. 4a). Both **1** and Tpe exhibit blue emission, 501 nm excited at 397 nm, and 455 nm excited at 378 nm, respectively. This luminescence properties of these compounds are due to the AIE effect from TPE-core^[24]. Compared to the emission peaks of Tpe, the emission peaks of **1** showed red-shift of 46 nm



(a)



(b)

Fig. 4. (a) Excitation and emission solid spectra of **1** (blue) and Tpe (red). (b) CIE coordinates of **1** (blue) and Tpe (red)

According to analysis of the above structures, the interaction sites and porous nature of **1** provide a feasible method for interaction with guest molecules, so the chemical sensing properties of compound **1** were further studied^[27]. The stability of compound **1** in different solvents was researched (Fig. S2). Solvent exchange was carried out at room temperature by soaking compound **1** in solvents for 24 hours with fresh solvents replenished every 4 hours. It is found that their structures are all intact, and the photoluminescence emission spectra of compound **1** in various solvents were also conducted at room temperature. Fluorescence tests after solvents exchange showed that **1** in non-aromatic solvents had its fluorescence intensity reduced (Fig. 5a)^[28, 29] because the adsorption of small molecules into the porous structure of **1** constrains the free rotation. In aromatic solvent molecules, the fluorescence is quenched by rotation. Studies have revealed that containing electron deficient groups like nitrobenzene quenches the emission of **1**, while that having electron donating groups like toluene shows an enhancing ability (Fig. S3). This phenomenon indicates that **1** has potential value as an organic solvent fluorescence sensor.

3.4 Selective sensing of cations and anions

Since **1** is structurally stable and strongly luminescent in water, it was investigated in the presence of metal cations. Activated **1** was immersed in aqueous solutions containing 10

(Fig. 4a). This emission band could be assigned to the emission of ligand-to-ligand charge transfer (LLCT)^[25]. And the weakened emission peak in **1** may be the result from the weakened conjugacy after coordination, which is similar to the reported complex $\{[(\text{sqpa})_2\text{Cd}(\text{bipy})(\text{H}_2\text{O})]_2 \cdot [\text{Cd}(\text{bipy})_2(\text{H}_2\text{O})_2] \cdot 2(\text{H}_2\text{O})\}_n$ ^[26]. The Commission International de l'Eclairage (CIE) coordinates of **1** and Tpe are (0.223, 0.377) and (0.175, 0.187), respectively (Fig. 4b)

mM M^{x+} ($\text{M}^{x+} = \text{K}^+, \text{Mn}^{2+}, \text{Ni}^{2+}, \text{Pb}^{2+}, \text{Al}^{3+}, \text{Co}^{2+}, \text{Cr}^{3+}, \text{Cu}^{2+}, \text{Na}^+, \text{Zn}^{2+}, \text{Fe}^{2+}$, and Fe^{3+}) to form suspensions. As shown in Fig. 5b, the luminescence intensities of **1** were almost quenched by the addition of Fe^{3+} ions, while other metal ions have slightly increased or decreased luminescence intensities, which signifies that **1** can sense Fe^{3+} ions selectively in water. The same procedure was carried out to investigate the sensing properties towards anions by using aqueous solutions (Fig. 5d). Obviously, most anions have no significant fluorescence quenching effect on emission intensity except $\text{Cr}_2\text{O}_7^{2-}$ ions. Therefore, **1** can also be used as a light-emitting sensor to detect $\text{Cr}_2\text{O}_7^{2-}$ ions in aqueous solution.

Furthermore, the experiment of anti-interference sensing ability towards Fe^{3+} ions was also carried out (Fig. 5c). The equivalent sample **1** dispersed in different aqueous solutions of metal ions before the addition of Fe^{3+} ions. The results showed that the fluorescence intensity was significantly quenched once Fe^{3+} ions were introduced into an aqueous solution with other co-existing cations, indicating that the quenching induced by Fe^{3+} ions was not affected by other co-existing cations. Based on previous researches, the mechanism of luminescence quenching caused by Fe^{3+} ions may be as follows: i) the absorption of excitation/emission of the MOFs by Fe^{3+} ; ii) the interaction between Fe^{3+} ions and the organic ligands^[30].

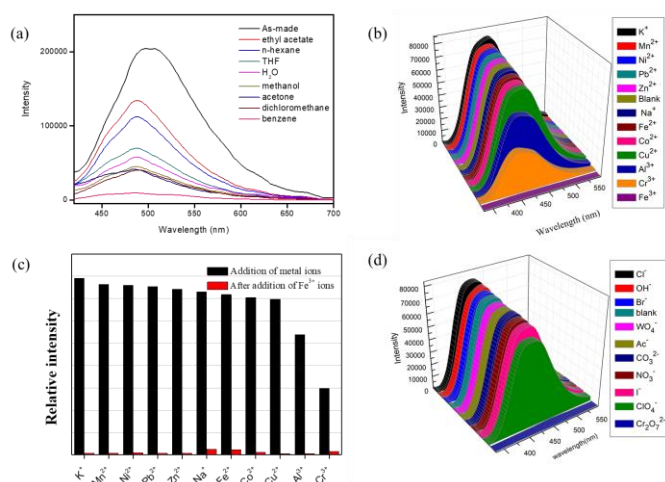


Fig. 5. (a) Fluorescence spectra of **1** dispersed in different solvents. (b) Fluorescence intensities of **1** in the presence of different metal ions. (c) Black represents the luminescence intensities when different metal ions are present. Red represents the change in the emission after adding Fe³⁺ ions. (d) Luminescence intensities of **1** dispersed in the aqueous solutions of different anions

4 CONCLUSION

In summary, a novel Cd based luminescent metal-organic framework (LMOF), $[\text{Cd}_3(\text{Tipe})_{1.5}(\text{bpodc})_2\text{Cl}_2](\text{H}_2\text{O})_2)_n$, was successfully synthesized by a tetraphenylethene (TPE)-core ligand under hydrothermal conditions. The structure of **1** was confirmed, its thermal stabilities, luminescence properties and sensing properties for cations and anions were also studied. Furthermore, compound **1** exhibits strong blue

emission in the solid state due to its TPE-core chromophore Tipe, which means **1** may be useful to the development of fluorescent materials. Solvent exchange experiments show that **1** is stable in most organic solvents. Moreover, **1** is a multi-responsive luminescent sensor for the detection of Fe³⁺ and Cr₂O₇²⁻ ions in aqueous solution selectively. More importantly, the sensor quenching Fe³⁺ ions are not affected by other cations.

REFERENCES

- (1) Zhao, S. N.; Zhang, Y.; Song, S. Y.; Zhang, H. J. Design strategies and applications of charged metal organic frameworks. *Coordin. Chem. Rev.* **2019**, 398, 113007.
- (2) Chen, L. Z.; Pan, Q. J.; Cao, X. X.; Wang, F. M. Crystal structure, magnetism, and dielectric properties based on the axially chiral ligand 2,2'-dinitro-4,4'-biphenyldicarboxylic acid. *Crystengcomm.* **2016**, 18, 1944–1952.
- (3) Pettinari, C.; Tabacaru, A.; Galli, S. Coordination polymers and metal-organic frameworks based on poly(pyrazole)-containing ligands. *Coordin. Chem. Rev.* **2016**, 307, 1–31.
- (4) Yan, X. Z.; Wang, M.; Cook, T. R.; Zhang, M. M.; Saha, M. L.; Zhou, Z. X.; Li, X. P.; Huang, F. H.; Stang, P. J. Light-emitting superstructures with anion effect: coordination-driven self-assembly of pure tetraphenylethylene metallacycles and metallacages. *J. Am. Chem. Soc.* **2016**, 138, 4580–4588.
- (5) Qin, Z. W.; Wang, Y.; Lu, X. F.; Chen, Y. J.; Peng, J.; Zhou, G. Multistimuli-responsive luminescence switching of pyrazine derivative based donor-acceptor-donor luminophores. *Chem. Asian J.* **2016**, 11, 285–293.
- (6) Liu, G. G.; Chen, D. D.; Kong, L. W.; Shi, J. B.; Tong, B.; Zhi, J. G.; Feng, X.; Dong, Y. P. Red fluorescent luminogen from pyrrole derivatives with aggregation-enhanced emission for cell membrane imaging. *Chem. Commun.* **2015**, 51, 8555–8558.
- (7) Lustig, W. P.; Li, J. Luminescent metal-organic frameworks and coordination polymers as alternative phosphors for energy efficient lighting devices. *Coordin. Chem. Rev.* **2018**, 373, 116–147.
- (8) Rudd, N. D.; Wang, H.; Teat, S. J.; Li, J. A dual linker metal-organic framework demonstrating ligand-based emission for the selective detection of carbon tetrachloride. *Inorg. Chim. Acta* **2018**, 470, 312–317.

- (9) Zhang, D. Y.; He, H. M.; Zhang, Y.; Wang, X. G.; Zhao, X. J.; Yang, E. C. A fluorescent zinc(II)-based layered complex for selective sensing of $\text{Cr}_2\text{O}_7^{2-}$ and Fe^{3+} ions in water system. *Indian J. Chem. B* **2019**, 58, 9–17.
- (10) Zhang, Y. Q.; Blatov, V. A.; Zheng, T. R.; Yang, C. H.; Qian, L. L.; Li, K.; Li, B. L.; Wu, B. A luminescent zinc(II) coordination polymer with unusual (3,4,4)-coordinated self-catenated 3D network for selective detection of nitroaromatics and ferric and chromate ions: a versatile luminescent sensor. *Dalton Trans.* **2018**, 47, 6189–6198.
- (11) Mako, T. L.; Racicot, J. M.; Levine, M. Supramolecular luminescent sensors. *Chem. Rev.* **2019**, 119, 322–477.
- (12) Pourmara, A. D.; Margariti, A.; Tarlas, G. D.; Kourtellaris, A.; Petkov, V.; Kokkinos, C.; Economou, A.; Papaefstathiou, G. S.; Manos, M. J. A Ca^{2+} MOF combining highly efficient sorption and capability for voltammetric determination of heavy metal ions in aqueous media. *J. Mater. Chem. A* **2019**, 7, 15432–15443.
- (13) Wang, J. J.; Cao, Z.; Tang, L.; Wang, X.; Hou, X. Y.; Ju, P.; Ren, Y. X. Synthesis, structure, photoluminescence and photocatalytic properties of a new Cd(II) metal-organic framework based on 1,4-di(2,6-dimethyl-3,5-dicarboxypyridyl)benzene. *Chin. J. Struct. Chem.* **2018**, 37, 1323–1330.
- (14) Jiang, B.; Zhang, C. W.; Shi, X. L.; Yang, H. B. AIE-active metal-organic coordination complexes based on tetraphenylethylene unit and their applications. *Chin. J. Polym. Sci.* **2019**, 37, 372–382.
- (15) Li, Q. Y.; Ma, Z.; Zhang, W. Q.; Xu, J. L.; Wei, W.; Lu, H.; Zhao, X. S.; Wang, X. J. AIE-active tetraphenylethylene functionalized metal-organic framework for selective detection of nitroaromatic explosives and organic photocatalysis. *Chem. Commun.* **2016**, 52, 11284–11287.
- (16) Li, W.; Ding, Y.; Tebyetekerwa, M.; Xie, Y.; Wang, L.; Li, H.; Hu, R.; Wang, Z.; Qin, A.; Tang, B. Z., Fluorescent aggregation-induced emission (AIE)-based thermosetting electrospun nanofibers: fabrication, properties and applications. *Mater. Chem. Front.* **2019**, 3, 2491–2498.
- (17) Yao, W.; Tebyetekerwa, M.; Bian, X.; Li, W.; Yang, S.; Zhu, M.; Hu, R.; Wang, Z.; Qin, A.; Tang, B. Z. Materials interaction in aggregation-induced emission (AIE)-based fluorescent resin for smart coatings. *J. Mater. Chem. C* **2018**, 6, 12849–12857.
- (18) Xu, X. D.; Liang, Y.; Mensah, A.; Li, J. F.; Zhou, L.; Chen, L. Z.; Wang, F. M. Synthesis, structures and fluorescence properties of two novel cadmium MOFs based on a tetraphenylethylene (TPE)-core ligand. *ChemistrySelect.* **2019**, 4, 12380–12385.
- (19) Wang, F. M.; Zhou, L.; Lustig, W. P.; Hu, Z.; Li, J. F.; Hu, B. X.; Chen, L. Z.; Li, J. Highly luminescent metal-organic frameworks based on an aggregation-induced emission ligand as chemical sensors for nitroaromatic compounds. *Cryst. Growth Des.* **2018**, 18, 5166–5173.
- (20) Li, J. F.; Xu, X. D.; Zhou, Z. Y.; Chen, L. Z.; Wang, F. M. Crystal structures and luminescent properties of a cadmium(II) metal-organic framework based on tri(4-pyridylphenyl)amine. *J. Coord. Chem.* **2018**, 71, 4023–4030.
- (21) Wang, F. M.; Zhou, Z. Y.; Liu, W.; Zhou, L.; Chen, L. Z.; Li, J. Two blue-light excitable yellow-emitting LMOF phosphors constructed by triangular tri(4-pyridylphenyl)amine. *Dalton Trans.* **2017**, 46, 956–961.
- (22) Kim, K. Y.; Jung, S. H.; Lee, J. H.; Lee, S. S.; Jung, J. H. An imidazole-appended *p*-phenylene-Cu(II) ensemble as a chemoprobe for histidine in biological samples. *Chem. Commun. (Camb)* **2014**, 50, 15243–6.
- (23) Wang, Y.; Yuan, B.; Xu, Y. Y.; Wang, X. G.; Ding, B.; Zhao, X. J. Turn-on fluorescence and unprecedented encapsulation of large aromatic molecules within a manganese(II)-triazole metal-organic confined space. *Chem. Eur. J.* **2015**, 21, 2107–2116.
- (24) Zhang, H. L.; Zhao, B.; Yuan, W. G.; Tang, W.; Xiong, F.; Jing, L. H.; Qin, D. B. Syntheses and characterizations of two-dimensional polymers based on tetraimidazole tetraphenylethylene ligand with aggregation-induced emission property. *Inorg. Chem. Commun.* **2013**, 35, 208–212.
- (25) Wang, F. M.; Liu, W.; Teat, S. J.; Xu, F.; Wang, H.; Wang, X. L.; An, L. T.; Li, J. Chromophore-immobilized luminescent metal-organic frameworks as potential lighting phosphors and chemical sensors. *Chem. Commun.* **2016**, 52, 10249–10252.
- (26) Feng, X.; Liu, J.; Li, J.; Ma, L. F.; Wang, L. Y.; Ng, S. W.; Qin, G. Z. Series of coordination polymers based on 4-(5-sulfo-quinolin-8-yloxy) phthalate and bipyridinyl coligands: Structure diversity and properties. *J. Solid State Chem.* **2015**, 230, 80–89.
- (27) Fu, R. B.; Hu, S. M.; Wu, X. T. Rapid and sensitive detection of nitroaromatic explosives by using new 3D lanthanide phosphonates. *J. Mater. Chem. A* **2017**, 5, 1952–1956.
- (28) Das, P.; Mandal, S. K. A highly emissive fluorescent Zn-MOF: molecular decoding strategies for solvents and trace detection of dunnite in water. *J. Mater. Chem. A* **2018**, 6, 21274–21279.
- (29) Wang, D.; Hu, Z.; Xu, S.; Li, D.; Zhang, Q.; Ma, W.; Zhou, H.; Wu, J.; Tian, Y. Fluorescent metal-organic frameworks based on mixed organic ligands: new candidates for highly sensitive detection of TNP. *Dalton Trans.* **2019**, 48, 1900–1905.
- (30) Guo, X. Y.; Dong, Z. P.; Zhao, F.; Liu, Z. L.; Wang, Y. Q. Zinc(II)-organic framework as a multi-responsive photoluminescence sensor for efficient and recyclable detection of pesticide 2,6-dichloro-4-nitroaniline, Fe(III) and Cr(VI). *New. J. Chem.* **2019**, 43, 2353–2361.